

One-Tube Nested PCR Coupled with CRISPR-Cas12a for Ultrasensitive Nucleic Acid Testing

Yugan He,[#] Yadan Peng,[#] and Yigang Tong^{*}Cite This: *ACS Omega* 2024, 9, 39616–39625

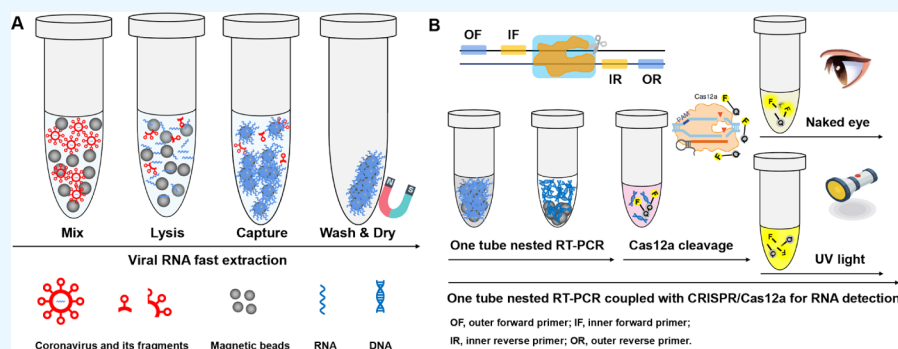
Read Online

ACCESS |

Metrics & More

Article Recommendations

Supporting Information



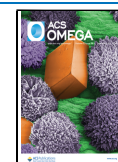
ABSTRACT: Nucleic acid testing with high sensitivity and specificity is of great importance for accurate disease diagnostics. Here, we developed an in situ one-tube nucleic acid testing assay. In this assay, the target nucleic acid is captured using magnetic silica beads, avoiding an elution step, followed directly by the polymerase chain reaction (PCR) and clustered regularly interspaced short palindromic repeats (CRISPR)-Cas12a detection. This assay achieved visual readout and a sensitivity of 120 copies/mL for detecting SARS-CoV-2. More importantly, the assay demonstrated over 95% sensitivity and 100% specificity compared to the gold standard real-time quantitative PCR (RT-qPCR) test by using 75 SARS-CoV-2 clinical samples. By integrating nested PCR and Cas12a, this all-in-one nucleic acid testing approach enables ultrasensitive, highly specific, and cost-effective diagnosis at community clinics and township hospitals.

1. INTRODUCTION

Coronavirus disease 2019 (COVID-19), caused by severe acute respiratory syndrome coronavirus 2 (SARS-CoV-2), remains a global health threat because of its high transmissibility and rapid spread.^{1,2} Symptoms of SARS-CoV-2 infections vary from mild influenza-like illness to severe, necessitating the development of highly sensitive early detection assays.^{3–5} Various SARS-CoV-2 detection methods exist.⁶ Antigen detection, often paired with lateral flow assays (LFA), can identify the N and E proteins.⁷ Although rapid and user-friendly for self-testing, most antigen detection lacks sensitivity. Serological assays, which detect IgM/IgG antibodies in serum via LFA,^{8,9} are typically used as supplementary tests because antibodies are detectable 1 week postinfection.¹⁰ Conversely, viral nucleic acid testing, known for its high specificity and sensitivity, is crucial for SARS-CoV-2 containment, as emphasized by the WHO.^{11,12} Key nucleic acid amplification tests (NAATs) include the polymerase chain reaction (PCR), isothermal amplification tests (IATs), and clustered regularly interspaced short palindromic repeats (CRISPR)-based methods. PCR, especially real-time quantitative PCR (RT-qPCR), is the benchmark for detection because of its precision and sensitivity.^{13–15} However, RT-qPCR

requires specialized personnel and equipment, making it costly, time-intensive, and inaccessible for resource-limited healthcare settings.¹¹

Nucleic acid-based IATs,^{16,17} such as transcription-mediated amplification (TMA),¹⁸ loop-mediated isothermal amplification (LAMP),¹⁹ recombinase polymerase amplification (RPA),^{20,21} and exponential amplification reaction (EXPAR),²² are PCR alternatives.²³ LAMP, however, is susceptible to contamination because of rapid amplification. Further, its sensitivity to very low viral loads is inferior to PCR assays.^{24,25} RPA, introduced in 2006 and advanced by TwistDx,^{26,27} can detect SARS-CoV-2 down to a few copies per reaction, matching the limit of detection (LOD) of RT-qPCR.²⁸ Nevertheless, RPA is expensive, requiring complex proteins and chemical probes.^{29,30}

Received: April 24, 2024**Revised:** July 28, 2024**Accepted:** August 14, 2024**Published:** September 13, 2024

Recently, CRISPR associated (Cas) systems, combined with nucleic acid amplification technologies like LAMP, RPA, or PCR, have emerged for pathogen detection.^{5,31–35} For instance, Guo et al. achieved a LOD of 1×10^4 copies/mL using recombinase-aided amplification (RAA) with CRISPR-Cas12a.³⁶ Similarly, Broughton et al. reached the same LOD combining LAMP with CRISPR-Cas12a and readout by LFA.³⁷ Fozouni et al. developed an amplification-free nucleic acid detection with CRISPR-Cas13a and smartphone readout, achieving a LOD of 1×10^5 copies/mL.³⁸ However, these CRISPR-integrated methods are less sensitive than qPCR. Recently, Ali et al. reported a single-tube RT-LAMP coupled with CRISPR-Cas12a system that had a LOD of 10 copies/reaction, which is higher than that of qPCR (5 copies/reaction).³⁹ Thus, an ideal diagnostic method would combine the sensitivity and specificity of nucleic acid amplification with the efficiency and stability of CRISPR, making this promising research direction for ultrasensitive nucleic acid detection.^{13,40}

In this study, we presented an ultrasensitive, visible (to the naked eye) nucleic acid test combining magnetic beads (MBs)-based RNA purification with a one-tube nested PCR/CRISPR-Cas12a system. We first assessed the compatibility of the PCR with MBs, then optimized the nested PCR/CRISPR-Cas12a system. Further, we evaluated 75 SARS-CoV-2 clinical samples using our developed method. Notably, the method does not require large instruments or centralized laboratories, making it suitable for primary healthcare in small communities.

2. EXPERIMENTAL SECTION

2.1. Materials. Primers, probes, and CRISPR RNA (crRNA) were synthesized by Ruibo Biotech (Beijing, China) (Table S1). Sodium hydroxide (NaOH), sodium chloride (NaCl), hydrochloric acid (HCl), and anhydrous ethanol were sourced from Macklin Biochemical (Shanghai, China). Ethylenediaminetetraacetic acid disodium salt (EDTA-Na₂), guanidine thiocyanate (GuSCN/C2H6N4S), and hydroxymethyl aminomethane (Tris) buffer were obtained from Solarbio Life Sciences (Beijing, China). Phosphate-buffered saline (PBS, 0.0067 M, pH7.4, Ca/Mg-free) was obtained from BI Biological Industries (Beijing, China). Ultrapure water ($18.2 \text{ M}\Omega \cdot \text{cm}$ at 25 °C) was produced with a Milli-Q reference system. The lysis buffer for nucleic acid extraction contained 2.5 mM EDTA, 20 mM Tris, 4 M GuSCN, and 2 M NaCl at pH 6. Silicon-hydroxyl (Si-OH) MBs (25 mg/mL) were obtained from Puri Mag Biotech (Xiamen, China). Mineral oil was purchased from Sigma-Aldrich (St. Louis, MO, USA). The SuperRT One-Step RT-PCR Kit and 50 × TAE buffer were obtained from CoWin Biosciences (Beijing, China). EnGen Lba Cas12a (Cpf1) and NEB buffer 2.1 were purchased from New England Biolabs (NEB, USA). The QIAamp Viral RNA Mini Kit was from QIAGEN (Hilden, Germany). The One-Step TB Green PrimeScript RT-PCR Kit (Perfect Real Time) was obtained from Takara (Dalian, China). Regular agarose G-10 was from Bioweste (Spain). Genecolour nucleic acid dye and DNA loading buffer (6×) were obtained from GeneBio and TransGen Biotech (Beijing, China), respectively, whereas RB2000 DNA markers were obtained from Ruibo Biotech (Beijing, China). The Qubit dsDNA HS Assay Kit was from Thermo Fisher Scientific (USA). GX/P2 V betacoronavirus⁴¹ was isolated from Vero E6 cells.

2.2. Nucleic Acid Extraction. The GX/P2 V coronavirus, which shares over 85% nucleotide sequence similarity with

SARS-CoV-2,⁴¹ was utilized to assess the MBs-based RNA extraction method. The procedure involved: (1) mixing MBs (10 μL , 25 mg/mL) with lysis buffer in a 1.5 mL Eppendorf tube (Nonpyrogenic or DNase-/RNase-free); (2) adding samples, mixing, incubating at room temperature for 5 min, and agitating every 2 min; (3) centrifuging briefly (FRONTIER 5306, OHAUS, USA) and transferring to a magnetic rack (DynaMag-2, Thermo Fisher Scientific, USA); (4) discarding the supernatant on achieving transparency; (5) adding 80% ethanol (200 μL), standing for 30 s, and discarding the supernatant; (6) repeating step 5 and air-drying for 5 min to evaporate residual ethanol; and (7) adding PCR premixture for subsequent reactions. For comparison, SARS-CoV-2 RNA extraction was also performed using the QIAamp Viral RNA Mini Kit, as recommended by the US Centers for Disease Control and Prevention.

2.3. One-Tube Nested PCR Amplification. Nested PCR primers for the N and ORF1ab genes of GX/P2 V and SARS-CoV-2, respectively, were designed using NCBI/BLAST/Primer-BLAST. Inner amplicon lengths were 90–120 bp, and those of the outer amplicons were 200–450 bp. Note that the inner amplicon sequence is included in the outer amplicon sequence. The one-tube nested RT-PCR used the SuperRT One-Step RT-PCR Kit. The reaction mix (25 μL) included 2 × SuperRT OneStep Buffer (12.5 μL), 10 μM inner and outer primer sets (2 μL), SuperRT OneStep EnzymeMix (0.5 μL), and nuclease-free water (8–9 μL). This mix was combined with viral RNA on MBs, transferred to a 0.2 mL PCR tube, sealed with mineral oil, and amplified using a thermal cycler. The protocol was 45 °C for 15 min, 95 °C for 2 min, followed by 40 cycles of 94 °C for 30 s, 55 °C for 30 s, 72 °C for 30 s, and a final extension at 72 °C for 5 min, before cooling to 4 °C.

2.4. CRISPR-Cas12a Fluorescence Detection. CRISPR-Cas12a crRNA was designed via GPP sgRNA Designer (CRISPRko, broadinstitute.org). The inner PCR amplicon required a TTTN protospacer adjacent motif (PAM) sequence for Cas12a/crRNA complex efficiency. The Cas12a system (20 μL) included 20 nM EnGen Lba Cas12a, 5 μM ssDNA reporter, 100 nM crRNA, 10 × NEB buffer 2.1 (2 μL), and nuclease-free water (12 μL). PCR products were added to the above CRISPR mixture, incubated at 37 °C for 40 min, and fluorescence was detected using gel imaging or UV excitation. Alternatively, reactions were visualized under natural light with a smartphone.

2.5. Sensitivity and Specificity. Sensitivity was first assessed using SARS-CoV-2 RNA with five 10-fold serial dilutions (10^{-1} to 10^4 copies/ μL). Then, the LOD for the one-tube assay was determined using probit analysis with a SARS-CoV-2 plasmid solution (600 μL). The negative controls (NTCs) used nuclease-free water. Specificity was tested using GX/P2 V coronavirus spiked into negative swab samples at 1.0×10^5 copies/mL using a 600- μL aliquot.

2.6. Clinical Specimen Analysis. Seventy-five clinical samples were analyzed using the one-tube nested PCR/CRISPR-Cas12a assay. Forty-three positive specimens from the Wuhan Hospital and 32 negative oropharyngeal swabs from Tong Lab volunteers were tested.

2.7. Ethics Statement. In this study, our objective was to develop a rapid diagnostic assay for SARS-CoV-2 to facilitate the timely diagnosis of COVID-19. We utilized anonymized surplus samples originally collected for SARS-CoV-2 diagnostic testing to establish and validate our protocol. Ethical approval

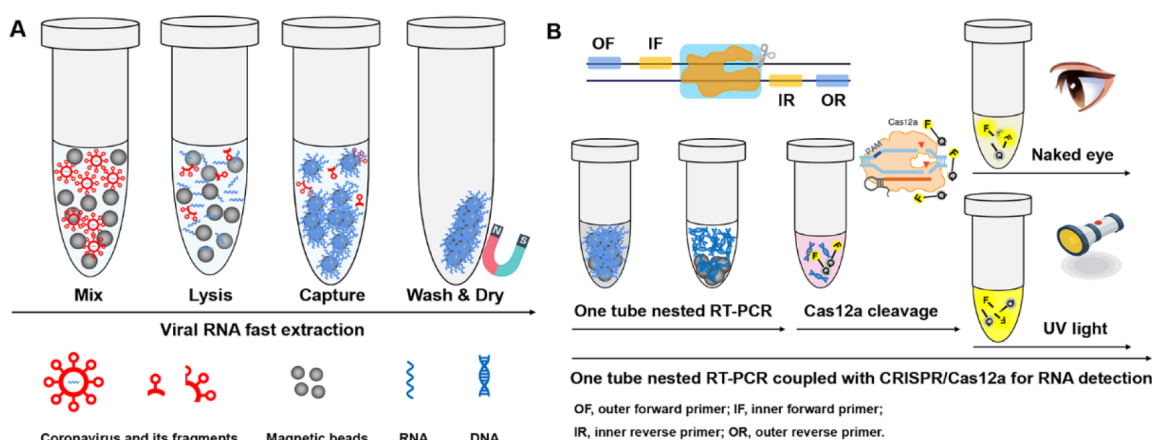


Figure 1. One-tube nested PCR/CRISPR-Cas12a assay schematic. (A) MBs-based viral RNA extraction and (B) assay with visual (fluorescence or naked eye) readout.

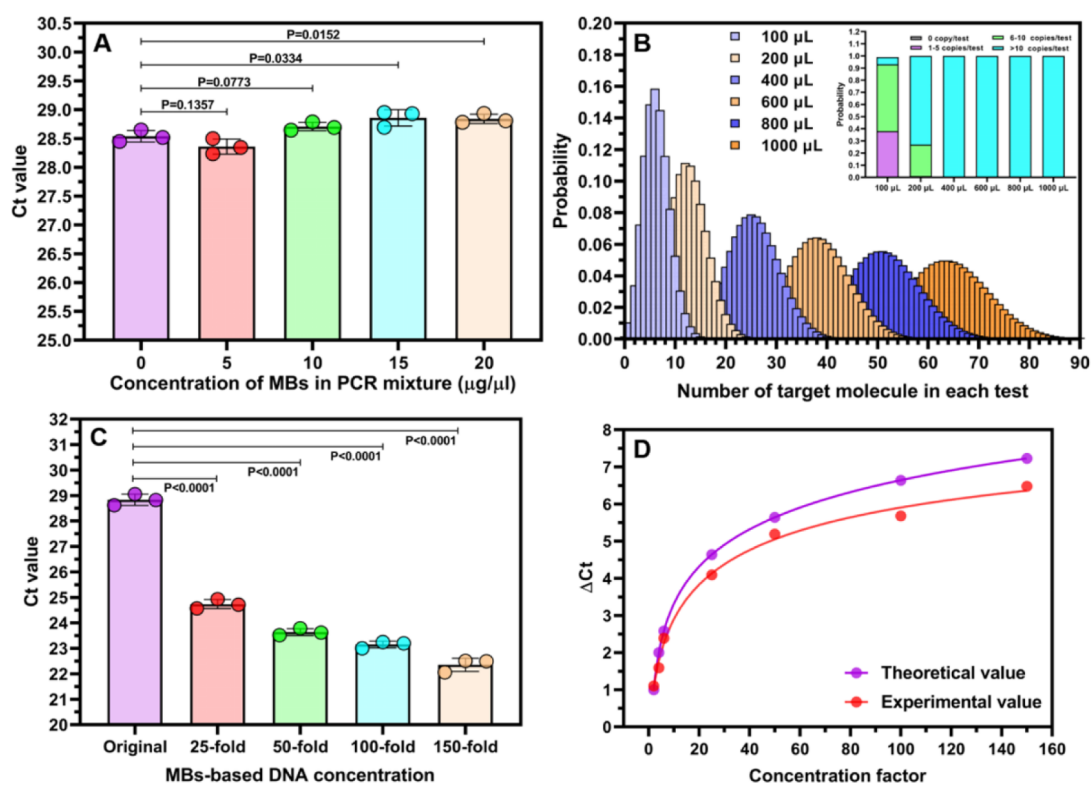


Figure 2. MBs tolerance of the PCR. (A) Tolerance across MBs concentrations, (B) Poisson distribution using different sample volumes, (C) qPCR Ct across sample volumes, and (D) ΔCt and concentration factor relationship, where $\Delta\text{Ct} = \text{Ct}_{\text{original}} - \text{Ct}_{\text{concentrated}}$ and concentration factor = $V_{\text{concentrated}}/V_{\text{original}}$.

for this study was granted by the Review Board of Beijing University of Chemical Technology. In accordance with ethical standards, informed consent was obtained from all participants involved in the study.

3. RESULTS

3.1. Construction of One-Tube Nested PCR-Cas12a Assay. An integrated visual nucleic acid test combining one-tube nested PCR with CRISPR-Cas12a was developed. As shown in Figure 1, viral RNA was purified and concentrated using MBs via an elution-free method. The enriched RNA on the MBs was directly mixed with the PCR mixture and sealed with mineral oil to avoid aerosol contamination. The resulted

PCR products were added to the Cas12a reaction mixture for detection. The CRISPR-Cas12a system includes a ssDNA reporter modified with a FAM fluorophore at the 5' end and a BHQ1 quencher at the 3' end. When the target was present, the *trans*-cleavage activity of Cas12a was activated and the ssDNA reporter was cut off. In the absence of the target, Cas12a showed no *trans*-cleavage activity on the ssDNA reporter. When the ssDNA FAM reporter was not cut by Cas12a, its high concentration resulted in the light pink coloration of the solution under natural light but no fluorescence signal under UV light excitation. When the ssDNA FAM reporter was cleaved, the solution changed from light pink to light yellow under natural light, and the FAM fluorescence signal was observed under UV light excitation.

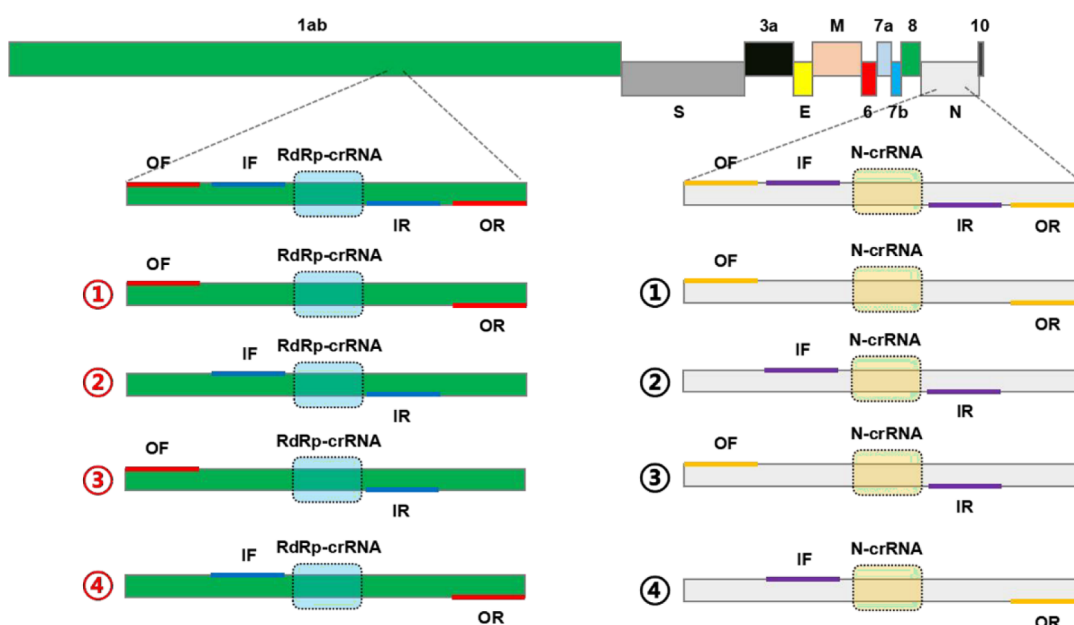


Figure 3. Nested PCR primer design. Four amplification modes per set, each including crRNA target sequence.

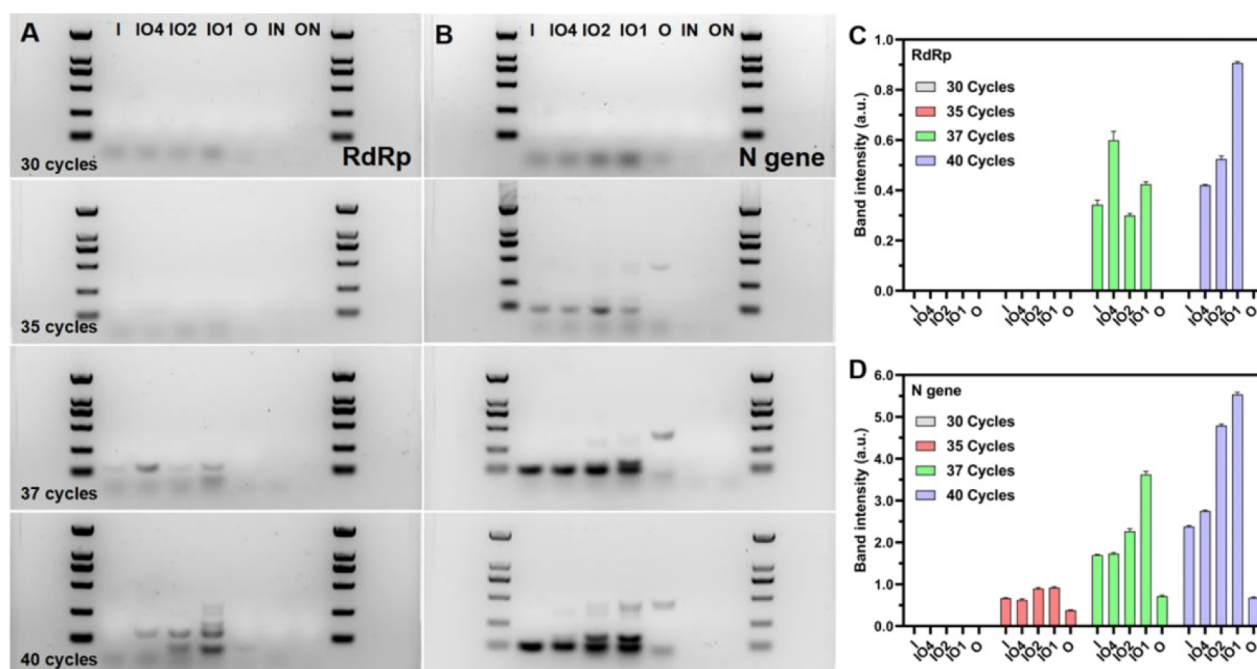


Figure 4. Inner/outer primer concentration optimization for nested PCR. (A, C) RdRp region and (B, D) N gene. The DNA fragments on the agarose gel electrophoresis bands were 100, 250, 500, 750, 1000, and 2000 bp from bottom to top. I, O, IO indicate inner primers, outer primers and nested primers, respectively. IN, and ON represent negative controls for I, and O, respectively. N indicates negative control with nuclease-free water instead of positive template. 4, 2, and 1 indicate inner: outer primer molar ratios of 4:1, 2:1, and 1:1, respectively.

Therefore, the results of the one-tube assay could be visualized based on the color change of the reaction solution under either natural or UV light.

3.2. One-Tube Nested PCR Amplification on MBs.

Because MBs are present in the PCR solution, we first investigated the tolerance of PCR amplification to the MBs. As shown in Figure 2A, with the increase in MBs concentration, the cycle threshold (Ct) value did not significantly decrease ($p < 0.05$), indicating that the introduction of MBs did not suppress the PCR. Sample input volume is critical for the development of highly sensitive and robust PCR assays. For

the PCR tests, the probability of sampling a given number of target molecules was calculated using Poisson distribution assuming various sample input volumes.^{42–44} For a sample having an indicated concentration of 100 copies/mL, sampling improved dramatically on increasing the sample input volume from 100 to 400 μL (Figure 2B). Interestingly, we also observed that 400 μL was sufficient for achieving robust one-tube nested PCR amplification, and there was no need to increase the sample input volume.

Next, at an indicated concentration of 7.8×10^2 copies/ μL , various volume of SARS-CoV-2 samples were concentrated

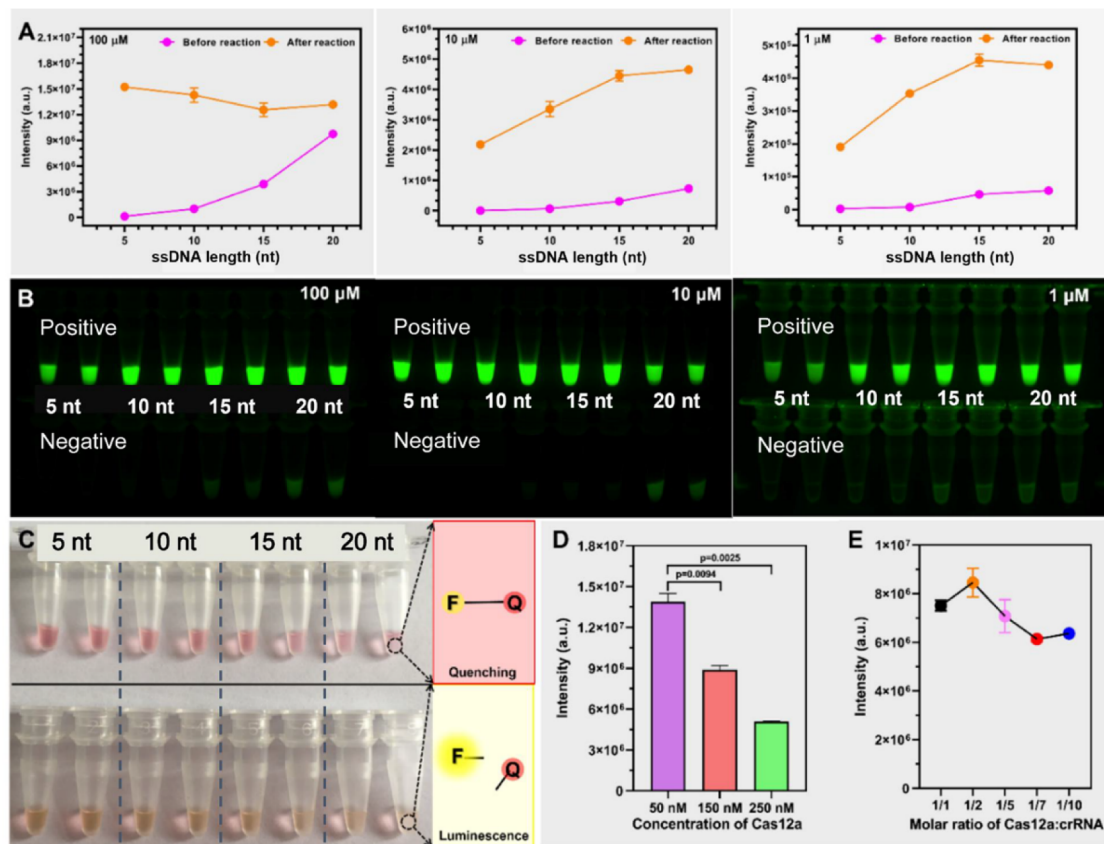


Figure 5. CRISPR Cas12a detection optimization. (A) ssDNA reporter effects, (B) UV end point images, (C) natural light detection, (D) Cas12a concentration effects, and (E) Cas12a/crRNA ratio effects.

using the MBs and then analyzed by one-tube nested PCR assay. As shown in Figure 2C, increased sample volume of 4 μL (original), 100 μL (25-fold), 200 μL (50-fold), 400 μL (100-fold), and 600 μL (150-fold) showed decreased Ct values of 28.83, 24.74, 23.64, 23.15, and 22.35, respectively. This result demonstrates that increasing sample input volume can effectively concentrate the target of interest, thus improving test sensitivity.

In addition, the relationship between ΔCt and the concentration factor was analyzed. As shown in Figure 2D, when the concentration factor is <6 , the theoretical ΔCt aligns with the experimental value. For instance, a sample concentrated 6-fold by MBs yields a theoretical ΔCt of 2.58 ($2^{2.58} \approx 5.98$, assuming PCR amplification efficiency is 100%), compared to an experimental ΔCt of 2.39 ($2^{2.39} \approx 5.24$). These results indicate that increasing the sample volume enhances PCR test sensitivity and robustness.

3.3. Screening of One-Tube Nested PCR Primers.

Primers are crucial for obtaining sensitive PCR assays. To target the ORF1ab and N genes of SARS-CoV-2, we first fixed the CRISPR-Cas12a crRNAs containing a 5' PAM sequence (TTTN). Figure 3 shows inner (IF and IR) and outer (OF and OR) PCR primers based on crRNA sequences. The nested structure amplifies more targets and prevents missed detection due to primer region variations. Nested PCR primer sets offer four amplification modes (OF/OR, IF/IR, OF/IR, IF/OR), each incorporating the crRNA target sequence.

Next, the nested PCR primers were evaluated for generating four distinct PCR products at different target concentrations (1:1 inner/outer primer ratio). Figure S1A,S1B shows that the

amplification effect of the outer primer was predominant at high target concentrations, followed by those of the inner primer and their combinations (RdRp target >78 copies/ μL , N target >120 copies/ μL). At lower concentrations, the effect of the inner primer was slightly more pronounced. However, nested amplification, capable of simultaneous multiple product amplification, proved superior. Therefore, the nested primers IO3 and IO1, targeting RdRp and N genes, respectively, were chosen for their high efficiency in low-concentration samples.

The impact of inner/outer primer concentration ratios and cycle numbers on nested PCR was investigated. Figure 4A,C shows that electrophoretic analysis struggled to detect amplified fragments below 35 cycles at an RdRp concentration of 7.8 copies/ μL . Beyond 37 cycles, no bands appeared with inner or outer primers alone, whereas the nested primers produced clear bands and were more pronounced at 40 cycles. A 1:1 primer ratio yielded the most PCR products after 40 cycles.

Figure 4B,D shows no amplification below 30 cycles for a 12 copies/ μL SARS-CoV-2 N gene. However, products were detectable beyond 35 cycles, and the quantity increased with the increase in cycle number. Therefore, one-tube nested PCR was initially performed with a 1:1 ratio of inner and outer primers and 40 cycles of amplification.

Moreover, the CRISPR-Cas12a assay was employed to detect nested PCR products across varying cycle numbers and primer ratios. As shown in Figure S2, for the SARS-CoV-2 RdRp target (7.8 copies/ μL), no detection was noted at 30 PCR cycles with only the outer primer. However, detection was achieved using inner or nested primers. With the N gene

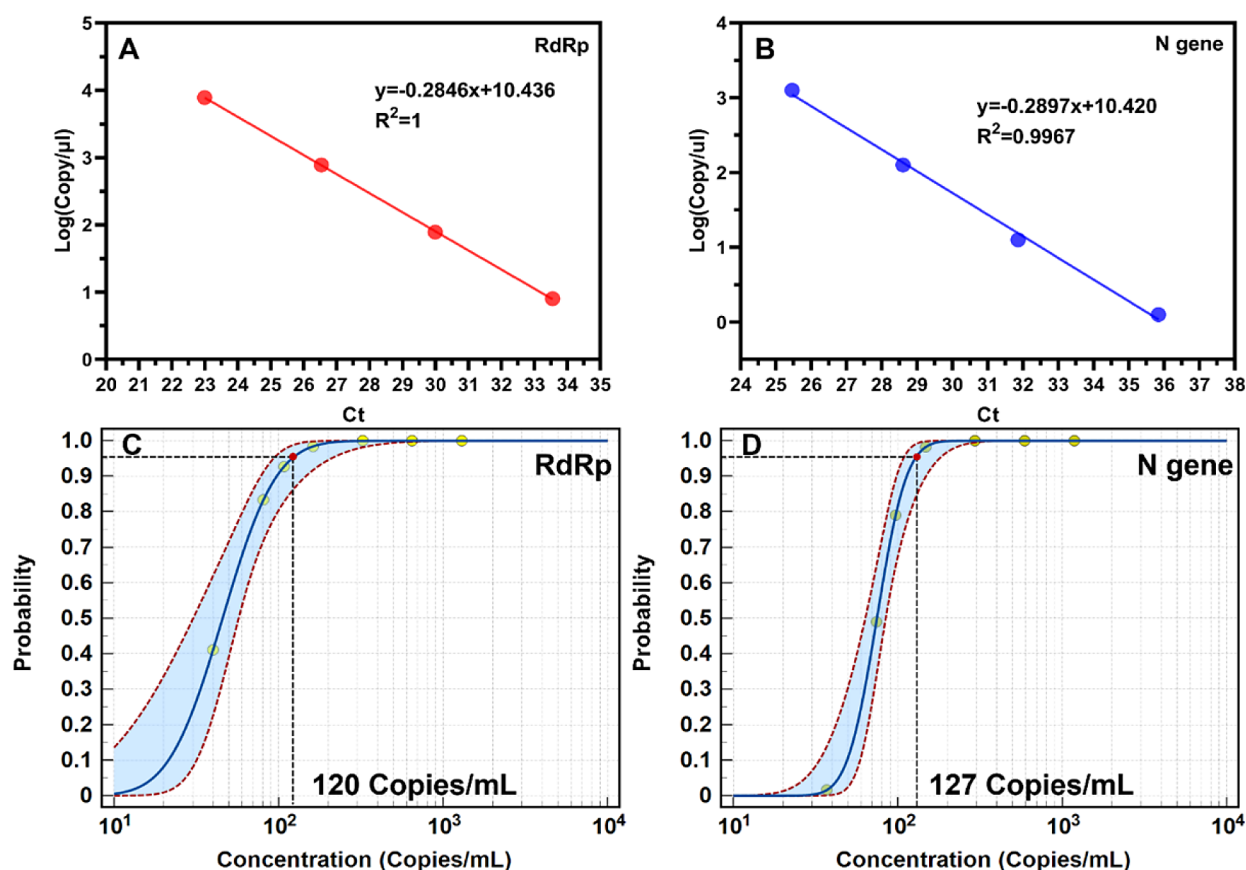


Figure 6. LOD for nested PCR/CRISPR-Cas12a assay. (A) RdRp region linearity curve, (B) N gene linearity curve, (C) RdRp region LOD, and (D) N gene LOD.

target (12 copies/ μL), CRISPR-Cas12a identified the PCR products at 30 cycles, demonstrating its heightened sensitivity for pathogen detection compared to electrophoretic analysis.

3.4. CRISPR-Cas12a Detection System Optimization.

Optimization of the CRISPR-Cas12a system involved assessing the ssDNA reporter length and concentration, as well as the crRNA and Cas12a concentrations. The background fluorescence intensity of the ssDNA reporter increased with the increase in length (5 to 20 nt) and concentration (Figure S3). Reporters shorter than 10 nt maintained low background fluorescence, even at high concentrations, peaking at 10×10^6 a.u. at $100 \mu\text{M}$. Longer reporters (over 15 nt) exhibited less quenching between 5' FAM and 3' BHQ1, leading to higher background fluorescence. After Cas12a cleavage, fluorescence intensity of reporters longer than 15 nt increased significantly at concentrations below $10 \mu\text{M}$. At $100 \mu\text{M}$, the high background masked changes postcleavage (Figure S4A,B). Therefore, the optimal ssDNA reporter length is below 10 nt, with 5 nt being ideal, within a concentration range of 1– $100 \mu\text{M}$. Color transitions from red to yellow post-Cas12a cleavage at $100 \mu\text{M}$ suggest that visual assessment is feasible (Figure 5C). As shown in Figure S4D,E, a Cas12a concentration of 50 nM, particularly with a 1:2 crRNA ratio, resulted in enhanced cleavage activity; thus, the optimal concentrations for Cas12a and crRNA were 50 and 100 nM, respectively.

Next, the optimized length of the ssDNA reporter of 5 nt was used, which yielded a light red color at 5– $7.5 \mu\text{M}$, turning light yellow after Cas12a cleavage, after which there were only subtle visual changes. For 10– $12.5 \mu\text{M}$, the color change was more distinct, indicating that $10 \mu\text{M}$ is the optimal

concentration for visual detection with CRISPR-Cas12a (Figure S4A). End point fluorescence imaging under UV excitation displayed a clear bright green for low-concentration ssDNA reporters, in contrast to the colorless NTC (Figure S4B). The detection of the SARS-CoV-2 RdRp target (7.8 copies/ μL) using one-tube nested PCR (40 cycles)/CRISPR-Cas12a showed positive real-time fluorescence at ssDNA reporter concentrations of 5– $12.5 \mu\text{M}$ (Figure S4C,D), indicating that assay results are easily interpretable without complex equipment and can be quickly obtained through real-time fluorescence or UV excitation. Moreover, three crRNAs targeting the SARS-CoV-2 RdRp region were designed, with crRNA3-Cas12a complexes showing the highest cleavage efficiency (Figure S5).

3.5. One-Tube Nested PCR-CRISPR 12a Assay Performance. The specificity of the one-tube nested PCR-Cas12a assay was confirmed using GX/P2 V simulated samples with SARS-CoV-2 RdRp/N gene-targeting primers and crRNAs.⁴¹ Stable detection of RdRp/N plasmids was observed, whereas GX/P2 V and the NTCs showed no detection (Figure S6A,S6B), demonstrating the high specificity of the assay without cross-reactivity.

Sensitivity was assessed with a SARS-CoV-2 RNA reference, achieving the detection of 1 copy/ μL of RdRp using any primer set, although the nested primers yielded more PCR products because of the increased fluorescence by CRISPR-Cas12a. For the N gene, the LOD was 10 copies/ μL with inner and outer primers and 1 copy/ μL with nested primers, indicating a 10-fold increase in sensitivity over conventional PCR/CRISPR-Cas12a (Figure S6C,D). We next evaluated the

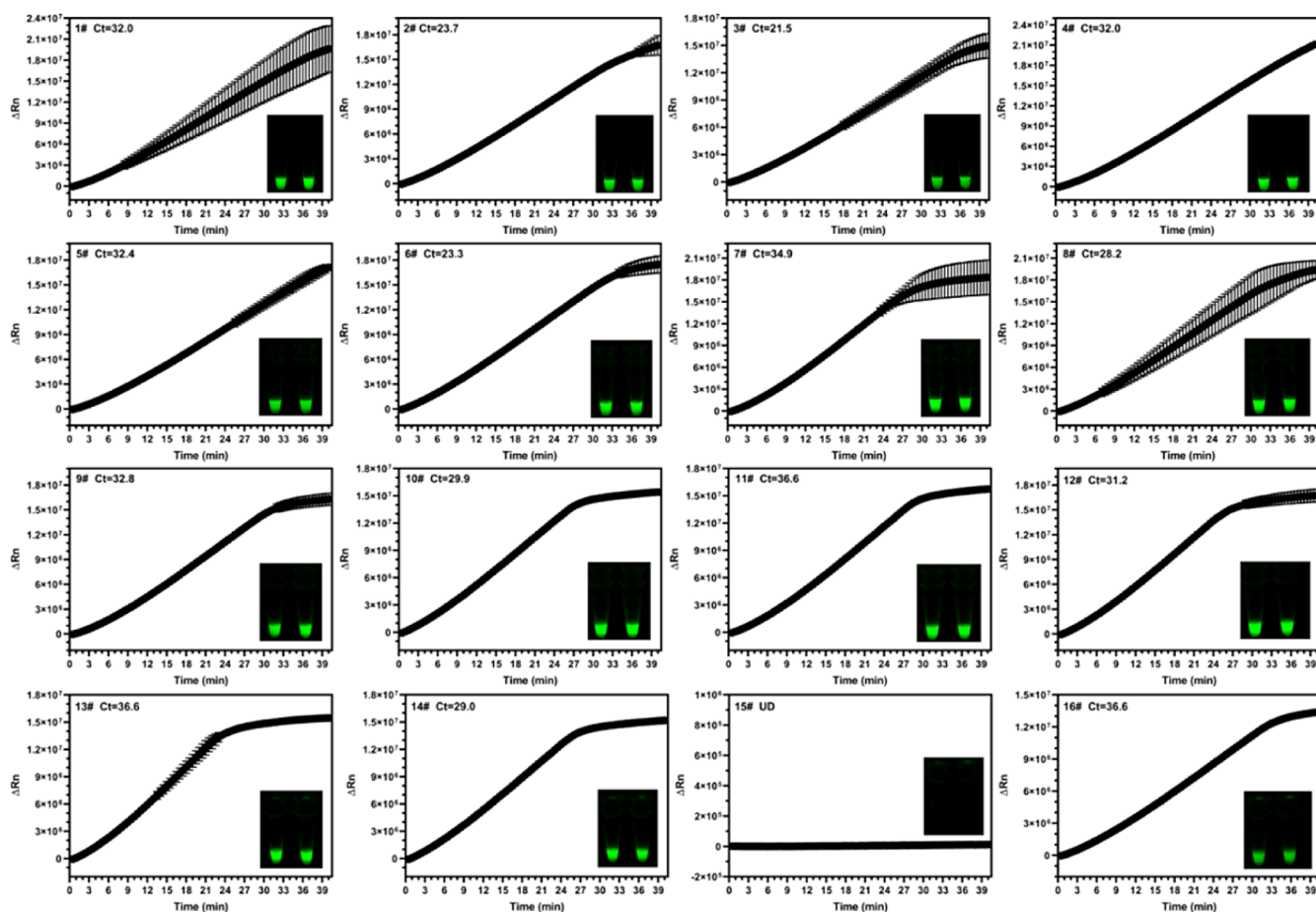


Figure 7. Real-time fluorescence results for nested PCR/CRISPR-Cas12a assay on clinical specimens.

amplification efficiency of nested PCR test (Figure 6A,B). For RdRp region detection, the amplification efficiency was 93%, and that for N gene was 95%. Then, LOD of the one-tube nested PCR/CRISPR-Cas12a assay was further evaluated using 600 μ L SARS-CoV-2 RdRp-/N-plasmid samples. The probit analysis results showed that LODs for RdRp region and N gene were 120 and 127 copies/mL, respectively (Figure 6C,D; Table S2).

It is crucial to detect mutant strains during pathogen identification. Therefore, we compared sequence variations between wild-type SARS-CoV-2 and five variants of concern (VOCs) in the PCR amplicon and CRISPR-Cas12a crRNA regions. Figure S7A shows that only the Beta variant exhibits a single “C” to “T” mutation at position 46 from the 5′ end in the RdRp amplicon. In contrast, the Delta and Omicron variants match the wild-type, indicating the conservation of RdRp and reliable hybridization of primers and crRNA with VOC sequences, thus avoiding misidentification. The N gene region of VOCs has up to ten mutations compared to the wild-type: five within the inner primer region; however, outer primer and crRNA regions are unaffected (Figure S7B–D). Notably, Delta and Omicron change the first three bases of the inner primer IF from “GGG” to “AAC”, but this minimally affects primer annealing and amplification initiation. Furthermore, primers OF and OR, OF and IR amplify effectively, ensuring no interference with the results. The precise pairing at the 3′ ends of the primers is crucial for the initiation of amplification by DNA polymerase. This analysis indicates that the one-tube nested PCR primers, which have multiple

amplification combinations, can mitigate the reduction in PCR products caused by mutations, thereby preventing off-target amplification of mutant strains.

3.6. Clinical Samples Validation. Lastly, we evaluated the performance of one-tube nested PCR/CRISPR-Cas12a assay using 75 clinical samples. As shown in Figure 7 (only 16 out of 75 clinical samples were presented here), results from real-time fluorescence analysis and end-point fluorescence image were the same, demonstrating that the real-time fluorescence analysis can be replaced by a much simpler end-point fluorescence image. Furthermore, a concordance analysis between nested PCR/CRISPR-Cas12a assay and RT-qPCR assay was performed. The results show that the one-tube nested PCR/CRISPR-Cas12a assay achieved 100% (Ct < 35) or 95% (Ct < 40) positive detection, and 100% negative detection compared to the gold standard RT-qPCR assay (Figure 8). Accordingly, the clinical sample validation confirmed the high sensitivity and specificity of the assay. Moreover, on targeting the RdRp/N genes, the assay achieved a 95.3% positive match rate (41/43) and a 96.9% negative match rate (31/32) for RdRp, and 95.3% positive (41/43) and 100% negative (32/32) for the N gene compared to RT-qPCR assay (Figures S8 and S9).

4. DISCUSSION

Emerging infectious pathogens such as SARS-CoV-2 and monkeypox virus have triggered a serious public health crisis worldwide. Highly specific and ultrasensitive detection platforms are indispensable for early pathogen diagnosis to contain

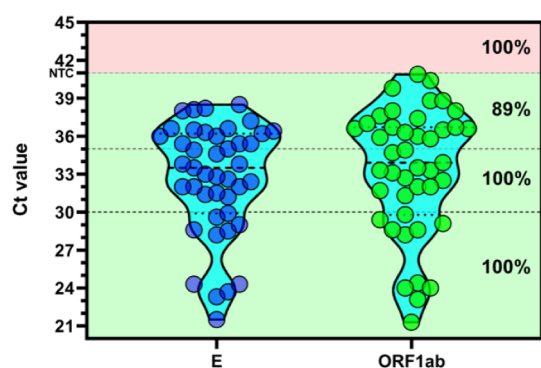


Figure 8. Concordance analysis between the one-tube nested PCR/CRISPR-Cas12a assay and the RT-qPCR assay.

the spread of contagious diseases efficiently. The gold standard RT-qPCR method is cumbersome and highly dependent on specialized operators and sophisticated qPCR instruments.⁴⁵ In recent years, many studies have demonstrated that CRISPR-based techniques combined with preamplification show great potential in developing accurate and sensitive nucleic acid detection.^{46,47}

Herein, we developed an all-in-one ultrasensitive and visible (to the naked eye) nucleic acid assay that combines an MBs-based extraction method with a nested PCR/CRISPR-Cas system. First, viral nucleic acids were concentrated by MBs directly from the original samples, thereby drastically simplifying the extraction process. This elution-free approach mitigates the shortcomings of conventional extraction methods due to the loss of target molecules.⁴⁸ Meanwhile, such an elution-free process minimizes the cross-contamination caused by sample transfer and centrifugation, and enables the advantages in large-scale purification.^{49,50} Increasing sample volume and using one-tube nested PCR are particularly beneficial for improving test sensitivity. Besides, the one-tube nested PCR providing multiple combination modes can effectively mitigate the loss of PCR products caused by mutations, thereby preventing off-target detection of mutant strains. The visual test results can be directly read by the naked eye, which not only significantly reduces the reliance on fluorescence readers but also makes the assay more accessible and user-friendly.

Ultimately, this assay achieved a LOD of 120 copies/mL, which is comparable to RT-qPCR, and is more sensitive than the one-pot RT-RPA/Cas12a assay (iSCAN-V2) (LOD: 8×10^3 copies/mL).⁵¹ The RPA assay is relatively more costly as it relies on multiple enzymes. Zhang et al. built a one-pot SNP assay using a LbCas12a variant with enhanced sensitivity (seCas12a), whereas our visible assay is more facile and applicable for detecting infectious diseases in resource-limited settings.⁵² Compared to currently reported RAA/CRISPR-Cas12a and LAMP/CRISPR-Cas12a/LFA assays (LOD: 1×10^4 copies/mL), our developed assay is more sensitive and cost-effective.^{36,37} Even though an RCA-coupled EXTRA-CRISPR assay offers a visual readout of the result, our assay shows a relatively high sensitivity.⁵³

Collectively, our one-tube visible ultrasensitive nested PCR/CRISPR-Cas assay excels in cost, convenience, specificity, sensitivity, intuitiveness, versatility, and robustness, promising significant advantages and immense development potential. We believe that this testing system will further promote the development of ultrasensitive, highly specific, and cost-effective

diagnostic strategies in community clinics and township hospitals.

5. CONCLUSION

We developed a streamlined visual nucleic acid assay integrating one-tube nested PCR with CRISPR-Cas12a detection. Viral RNA, purified with MBs, was directly used in one-tube nested PCR without prior RNA elution. The PCR product is detectable via CRISPR-Cas12a, and results are observable through colorimetric changes. Thus, this assay visually detects SARS-CoV-2 with a LOD of 120 copies/mL and reliably identifies various VOC mutants. Clinical evaluations demonstrated 95% positive and 100% negative agreement with RT-qPCR results. Overall, the one-tube nested PCR/CRISPR-Cas12a assay offers sensitivity and specificity comparable to qPCR, thus fulfilling the ultrasensitive nucleic acid detection requirements of community healthcare centers and rural clinics.

■ ASSOCIATED CONTENT

Supporting Information

The Supporting Information is available free of charge at <https://pubs.acs.org/doi/10.1021/acsomega.4c03911>.

Supplementary figures (Figures S1–S9), DNA and RNA sequences, and a comparison of various CRISPR-based nucleic acid testing methods (PDF)

■ AUTHOR INFORMATION

Corresponding Author

Yigang Tong – Beijing Advanced Innovation Center for Soft Matter Science and Engineering and College of Life Science and Technology, Beijing University of Chemical Technology, Beijing 100029, PR China; Email: tongyigang@mail.buct.edu.cn

Authors

Yugan He – Beijing Advanced Innovation Center for Soft Matter Science and Engineering and College of Life Science and Technology, Beijing University of Chemical Technology, Beijing 100029, PR China; Research & Development Department, Shenzhen New Industries Biomedical Engineering Co., Ltd, Shenzhen 518054, PR China; orcid.org/0000-0001-6583-4354

Yadan Peng – College of Life Science and Technology, Beijing University of Chemical Technology, Beijing 100029, PR China; orcid.org/0009-0001-8951-2349

Complete contact information is available at: <https://pubs.acs.org/10.1021/acsomega.4c03911>

Author Contributions

#Y.H. and Y.P. contributed equally to this work.

Notes

The authors declare no competing financial interest.

■ ACKNOWLEDGMENTS

This work was supported by Hebei Province Key Research and Development Program of China (No. 223777118D). We thank volunteers from Tong Lab for providing SARS-CoV-2 negative oropharyngeal swabs.

REFERENCES

- (1) Aburumman, A. A. COVID-19 impact and survival strategy in business tourism market: the example of the UAE MICE industry. *Humanit. Soc. Sci. Commun.* **2020**, *7* (1), 141.
- (2) Yang, Y.; Ruan, Q.; Huang, S.; Lan, T.; Wang, Y. Impact of the COVID-19 outbreak on tourists' real-time on-site emotional experience in reopened tourism destinations. *J. Hospitality And Tourism Manage.* **2021**, *48*, 390–394.
- (3) Panpradist, N.; Wang, Q.; Ruth, P. S.; Kotnik, J. H.; Oreskovic, A. K.; Miller, A.; Stewart, S. W. A.; Vrana, J.; Han, P. D.; Beck, I. A.; Starita, L. M.; Frenkel, L. M.; Lutz, B. R. Simpler and faster COVID-19 testing: Strategies to streamline SARS-CoV-2 molecular assays. *EBioMedicine* **2021**, *64*, 103236.
- (4) Guglielmi, G. Fast coronavirus tests: what they can and can't do. *Nature* **2020**, *585* (7826), 496–498.
- (5) Kaminski, M. M.; Abudayyeh, O. O.; Gootenberg, J. S.; Zhang, F.; Collins, J. J. CRISPR-based diagnostics. *Nat. Biomed. Eng.* **2021**, *5* (7), 643–656.
- (6) Esbin, M. N.; Whitney, O. N.; Chong, S.; Maurer, A.; Darzacq, X.; Tjian, R. Overcoming the bottleneck to widespread testing: a rapid review of nucleic acid testing approaches for COVID-19 detection. *RNA* **2020**, *26* (7), 771–783.
- (7) Aguilar-Shea, A. L.; Vera-García, M.; Güerri-Fernández, R. Rapid antigen tests for the detection of SARS-CoV-2: A narrative review. *Aten Primaria* **2021**, *53* (9), 102127.
- (8) Ku, Z.; Xie, X.; Hinton, P. R.; Liu, X.; Ye, X.; Muruato, A. E.; Ng, D. C.; Biswas, S.; Zou, J.; Liu, Y.; Pandya, D.; Menachery, V. D.; Rahman, S.; Cao, Y. A.; Deng, H.; Xiong, W.; Carlin, K. B.; Liu, J.; Su, H.; Haanes, E. J.; Keyt, B. A.; Zhang, N.; Carroll, S. F.; Shi, P. Y.; An, Z. Nasal delivery of an IgM offers broad protection from SARS-CoV-2 variants. *Nature* **2021**, *595* (7869), 718–723.
- (9) Ehrenstein, M. R.; Notley, C. A. The importance of natural IgM: scavenger, protector and regulator. *Nat. Rev. Immunol.* **2010**, *10* (11), 778–786.
- (10) Liu, Y.; Eggo, R. M.; Kucharski, A. J. Secondary attack rate and superspreading events for SARS-CoV-2. *Lancet* **2020**, *395* (10227), No. e47.
- (11) He, Y.; Wang, L.; An, X.; Tong, Y. All-in-one in situ colorimetric RT-LAMP assay for point-of-care testing of SARS-CoV-2. *Analyst* **2021**, *146* (19), 6026–6034.
- (12) Han, X.; Li, J.; Chen, Y.; Li, Y.; Xu, Y.; Ying, B.; Shang, H. SARS-CoV-2 nucleic acid testing is China's key pillar of COVID-19 containment. *Lancet* **2022**, *399* (10336), 1690–1691.
- (13) Carter, L. J.; Garner, L. V.; Smoot, J. W.; Li, Y.; Zhou, Q.; Saveson, C. J.; Sasso, J. M.; Gregg, A. C.; Soares, D. J.; Beskid, T. R.; Jervey, S. R.; Liu, C. Assay Techniques and Test Development for COVID-19 Diagnosis. *ACS Cent. Sci.* **2020**, *6* (5), 591–605.
- (14) Kang, T.; Lu, J.; Yu, T.; Long, Y.; Liu, G. Advances in nucleic acid amplification techniques (NAATs): COVID-19 point-of-care diagnostics as an example. *Biosens. Bioelectron.* **2022**, *206*, 114109.
- (15) LeBlanc, J. J.; Gubbay, J. B.; Li, Y.; Needle, R.; Arneson, S. R.; Marcino, D.; Charest, H.; Desnoyers, G.; Dust, K.; Fattouh, R.; Garceau, R.; German, G.; Hachette, T. F.; Kozak, R. A.; Krajden, M.; Kuschak, T.; Lang, A. L. S.; Levett, P.; Mazzulli, T.; McDonald, R.; Mubareka, S.; Prystajek, N.; Rutherford, C.; Smieja, M.; Yu, Y.; Zahariadis, G.; Zelyas, N.; Bastien, N. Real-time PCR-based SARS-CoV-2 detection in Canadian laboratories. *J. Clin. Virol.* **2020**, *128*, 104433.
- (16) Zhao, Y.; Chen, F.; Li, Q.; Wang, L.; Fan, C. Isothermal Amplification of Nucleic Acids. *Chem. Rev.* **2015**, *115* (22), 12491–12545.
- (17) De Felice, M.; De Falco, M.; Zappi, D.; Antonacci, A.; Scognamiglio, V. Isothermal amplification-assisted diagnostics for COVID-19. *Biosens. Bioelectron.* **2022**, *205*, 114101.
- (18) Brentano, S. T.; McDonough, S. H. Isothermal Amplification of RNA by Transcription-Mediated Amplification (TMA). In *Non-radioactive Analysis of Biomolecules*, Kessler, C., Eds.; Springer: Berlin Heidelberg, 2000; pp. 374380.
- (19) Notomi, T.; Okayama, H.; Masubuchi, H.; Yonekawa, T.; Watanabe, K.; Amino, N.; Hase, T. Loop-mediated isothermal amplification of DNA. *Nucleic Acids Res.* **2000**, *28* (12), No. e63.
- (20) Piepenburg, O.; Williams, C. H.; Stemple, D. L.; Armes, N. A. DNA detection using recombination proteins. *PloS Biol.* **2006**, *4* (7), No. e204.
- (21) Li, J.; Macdonald, J.; von Stetten, F. Review: a comprehensive summary of a decade development of the recombinase polymerase amplification. *Analyst* **2019**, *144* (1), 31–67.
- (22) Qian, J.; Ferguson, T. M.; Shinde, D. N.; Ramírez-Borrero, A. J.; Hintze, A.; Adami, C.; Niemz, A. Sequence dependence of isothermal DNA amplification via EXPAR. *Nucleic Acids Res.* **2012**, *40* (11), No. e87.
- (23) Carter, J. G.; Orueta Iturbe, L.; Duprey, J.-L. H. A.; Carter, I. R.; Southern, C. D.; Rana, M.; Whalley, C. M.; Bosworth, A.; Beggs, A. D.; Hicks, M. R.; Tucker, J. H. R.; Dafforn, T. R. Ultrarapid detection of SARS-CoV-2 RNA using a reverse transcription-free exponential amplification reaction, RTF-EXPAR. *Proc. Natl. Acad. Sci. U. S. A.* **2021**, *118* (35), No. e2100347118.
- (24) Kitajima, H.; Tamura, Y.; Yoshida, H.; Kinoshita, H.; Katsuta, H.; Matsui, C.; Matsushita, A.; Arai, T.; Hashimoto, S.; Iuchi, A.; Hirashima, T.; Morishita, H.; Matsuoka, H.; Tanaka, T.; Nagai, T. Clinical COVID-19 diagnostic methods: Comparison of reverse transcription loop-mediated isothermal amplification (RT-LAMP) and quantitative RT-PCR (qRT-PCR). *J. Clin. Virol.* **2021**, *139*, 104813.
- (25) Larremore, D. B.; Wilder, B.; Lester, E.; Shehata, S.; Burke, J. M.; Hay, J. A.; Tambe, M.; Mina, M. J.; Parker, R. Test sensitivity is secondary to frequency and turnaround time for COVID-19 screening. *Sci. Adv.* **2021**, *7* (1), No. eabd5393.
- (26) Daher, R. K.; Stewart, G.; Boissinot, M.; Bergeron, M. G. Recombinase Polymerase Amplification for Diagnostic Applications. *Clin. Chem.* **2016**, *62* (7), 947–958.
- (27) James, A.; Macdonald, J. Recombinase polymerase amplification: Emergence as a critical molecular technology for rapid, low-resource diagnostics. *Expert Rev. Mol. Diagn.* **2015**, *15* (11), 1475–1489.
- (28) Xia, S.; Chen, X. Single-copy sensitive, field-deployable, and simultaneous dual-gene detection of SARS-CoV-2 RNA via modified RT-RPA. *Cell Discov.* **2020**, *6* (1), 37.
- (29) Ahn, H.; Batule, B. S.; Seok, Y.; Kim, M.-G. Single-Step Recombinase Polymerase Amplification Assay Based on a Paper Chip for Simultaneous Detection of Multiple Foodborne Pathogens. *Anal. Chem.* **2018**, *90* (17), 10211–10216.
- (30) Li, J.; Pollak, N. M.; Macdonald, J. Multiplex Detection of Nucleic Acids Using Recombinase Polymerase Amplification and a Molecular Colorimetric 7-Segment Display. *ACS Omega* **2019**, *4* (7), 11388–11396.
- (31) Gootenberg, J. S.; Abudayyeh, O. O.; Lee, J. W.; Essletzbichler, P.; Dy, A. J.; Joung, J.; Verdine, V.; Donghia, N.; Daringer, N. M.; Freije, C. A.; Myhrvold, C.; Bhattacharyya, R. P.; Livny, J.; Regev, A.; Koonin, E. V.; Hung, D. T.; Sabeti, P. C.; Collins, J. J.; Zhang, F. Nucleic acid detection with CRISPR-Cas13a/C2c2. *Science* **2017**, *356* (6336), 438–442.
- (32) Myhrvold, C.; Freije, C. A.; Gootenberg, J. S.; Abudayyeh, O. O.; Metsky, H. C.; Durbin, A. F.; Kellner, M. J.; Tan, A. L.; Paul, L. M.; Parham, L. A.; Garcia, K. F.; Barnes, K. G.; Chak, B.; Mondini, A.; Nogueira, M. L.; Isern, S.; Michael, S. F.; Lorenzana, I.; Yozwiak, N. L.; MacInnis, B. L.; Bosch, I.; Gehrke, L.; Zhang, F.; Sabeti, P. C. Field-deployable viral diagnostics using CRISPR-Cas13. *Science* **2018**, *360* (6387), 444–448.
- (33) Chen, J. S.; Ma, E.; Harrington, L. B.; Da Costa, M.; Tian, X.; Palefsky, J. M.; Doudna, J. A. CRISPR-Cas12a target binding unleashes indiscriminate single-stranded DNase activity. *Science* **2018**, *360* (6387), 436–439.
- (34) Ganbaatar, U.; Liu, C. CRISPR-Based COVID-19 Testing: Toward Next-Generation Point-of-Care Diagnostics. *Front. Cell. Infect. Microbiol.* **2021**, *11*, 663949.

- (35) Li, S.-Y.; Cheng, Q.-X.; Wang, J.-M.; Li, X.-Y.; Zhang, Z.-L.; Gao, S.; Cao, R.-B.; Zhao, G.-P.; Wang, J. CRISPR-Cas12a-assisted nucleic acid detection. *Cell Discov.* **2018**, *4* (1), 20.
- (36) Guo, L.; Sun, X.; Wang, X.; Liang, C.; Jiang, H.; Gao, Q.; Dai, M.; Qu, B.; Fang, S.; Mao, Y.; Chen, Y.; Feng, G.; Gu, Q.; Wang, R. R.; Zhou, Q.; Li, W. SARS-CoV-2 detection with CRISPR diagnostics. *Cell Discov.* **2020**, *6* (1), 34.
- (37) Broughton, J. P.; Deng, X.; Yu, G.; Fasching, C. L.; Servellita, V.; Singh, J.; Miao, X.; Streithorst, J. A.; Granados, A.; Sotomayor-Gonzalez, A.; Zorn, K.; Gopez, A.; Hsu, E.; Gu, W.; Miller, S.; Pan, C.-Y.; Guevara, H.; Wadford, D. A.; Chen, J. S.; Chiu, C. Y. CRISPR-Cas12-based detection of SARS-CoV-2. *Nat. Biotechnol.* **2020**, *38* (7), 870–874.
- (38) Fozouni, P.; Son, S.; Diaz de Leon Derby, M.; Knott, G. J.; Gray, C. N.; D'Ambrosio, M. V.; Zhao, C.; Switz, N. A.; Kumar, G. R.; Stephens, S. I.; Boehm, D.; Tsou, C. L.; Shu, J.; Bhuiya, A.; Armstrong, M.; Harris, A. R.; Chen, P. Y.; Osterloh, J. M.; Meyer-Franke, A.; Joehnk, B.; Walcott, K.; Sil, A.; Langelier, C.; Pollard, K. S.; Crawford, E. D.; Puschnik, A. S.; Phelps, M.; Kistler, A.; DeRisi, J. L.; Doudna, J. A.; Fletcher, D. A.; Ott, M. Amplification-free detection of SARS-CoV-2 with CRISPR-Cas13a and mobile phone microscopy. *Cell* **2021**, *184* (2), 323–333 e9.
- (39) Ali, Z.; Aman, R.; Mahas, A.; Rao, G. S.; Tehseen, M.; Marsic, T.; Salunke, R.; Subudhi, A. K.; Hala, S. M.; Hamdan, S. M.; Pain, A.; Alofi, F. S.; Alsomali, A.; Hashem, A. M.; Khogeer, A.; Almontashiri, N. A. M.; Abedalthagafi, M.; Hassan, N.; Mahfouz, M. M. iSCAN: An RT-LAMP-coupled CRISPR-Cas12 module for rapid, sensitive detection of SARS-CoV-2. *Virus Res.* **2020**, *288*, 198129.
- (40) Yang, H.; Zhang, Y.; Teng, X.; Hou, H.; Deng, R.; Li, J. CRISPR-based nucleic acid diagnostics for pathogens. *Trends Analyt. Chem.* **2023**, *160*, 116980.
- (41) Lam, T. T.-Y.; Jia, N.; Zhang, Y.-W.; Shum, M.-H.-H.; Jiang, J.-F.; Zhu, H.-C.; Tong, Y.-G.; Shi, Y.-X.; Ni, X.-B.; Liao, Y.-S.; Li, W.-J.; Jiang, B.-G.; Wei, W.; Yuan, T.-T.; Zheng, K.; Cui, X.-M.; Li, J.; Pei, G.-Q.; Qiang, X.; Cheung, W. Y.-M.; Li, L.-F.; Sun, F.-F.; Qin, S.; Huang, J.-C.; Leung, G. M.; Holmes, E. C.; Hu, Y.-L.; Guan, Y.; Cao, W.-C. Identifying SARS-CoV-2-related coronaviruses in Malayan pangolins. *Nature* **2020**, *583* (7815), 282–285.
- (42) He, Y.; Xie, T.; Tu, Q.; Tong, Y. Importance of sample input volume for accurate SARS-CoV-2 qPCR testing. *Anal. Chim. Acta* **2022**, *1199*, 339585.
- (43) Zhang, Y.; Noji, H. Digital Bioassays: Theory, Applications, and Perspectives. *Anal. Chem.* **2017**, *89* (1), 92–101.
- (44) Yen, G. S.; Fujimoto, B. S.; Schneider, T.; Kreutz, J. E.; Chiu, D. T. Statistical Analysis of Nonuniform Volume Distributions for Droplet-Based Digital PCR Assays. *J. Am. Chem. Soc.* **2019**, *141* (4), 1515–1525.
- (45) Weissleder, R.; Lee, H.; Ko, J.; Pittet, M. J. COVID-19 diagnostics in context. *Sci. Transl. Med.* **2020**, *12* (546), No. eabc1931.
- (46) Paul, B.; Montoya, G. CRISPR-Cas12a: Functional overview and applications. *Biomed. J.* **2020**, *43* (1), 8–17.
- (47) Li, L.; Shen, G.; Wu, M.; Jiang, J.; Xia, Q.; Lin, P. CRISPR-Cas-mediated diagnostics. *Trends Biotechnol.* **2022**, *40* (11), 1326–1345.
- (48) Muir, P.; Nicholson, F.; Jhetam, M.; Neogi, S.; Banatvala, J. E. Rapid diagnosis of enterovirus infection by magnetic bead extraction and polymerase chain reaction detection of enterovirus RNA in clinical specimens. *J. Clin. Microbiol.* **1993**, *31* (1), 31–38.
- (49) Berensmeier, S.; Pisanic, N. Magnetic particles for separation and purification of nucleic acids. *Bio. Tech. Int.* **2007**, *73*, 495–504.
- (50) Akutsu, J.-I.; Tojo, Y.; Segawa, O.; Obata, K.; Okochi, M.; Tajima, H.; Yohda, M. Development of an integrated automation system with a magnetic bead-mediated nucleic acid purification device for genetic analysis and gene manipulation. *Biotechnol. Bioeng.* **2004**, *86* (6), 667–671.
- (51) Aman, R.; Marsic, T.; Sivakrishna Rao, G.; Mahas, A.; Ali, Z.; Alsanea, M.; Al-Qahtani, A.; Alhamlan, F.; Mahfouz, M. iSCAN-V2: A One-Pot RT-RPA–CRISPR/Cas12b Assay for Point-of-Care SARS-CoV-2 Detection. *Front Bioeng. Biotechnol.* **2022**, *9*, 800104.
- (52) Zhang, H.-X.; Zhang, C.; Lu, S.; Tong, X.; Zhang, K.; Yin, H.; Zhang, Y. Cas12a-based one-pot SNP detection with high accuracy. *Cell Insight* **2023**, *2* (2), 100080.
- (53) Yan, H.; Wen, Y.; Tian, Z.; Hart, N.; Han, S.; Hughes, S. J.; Zeng, Y. A one-pot isothermal Cas12-based assay for the sensitive detection of microRNAs. *Nat. Biomed. Eng.* **2023**, *7* (12), 1583–1601.